UNIVERSITÉ DU BURUNDI
GRENIER DU SAVOIR DU BURUNDI
Dépôt institutionnel officiel
https://repository.ub.edu.bi

Two-Aircraft Dynamic System on Approach. Flight Path and noise Optimization

Nahayo, Fulgence; Khardi, Salah; Haddou, Mounir

2012
ResearchGate
https://repository.ub.edu.bi/handle/123456789/1301

Document téléchargé depuis le **Grenier du Savoir du Burundi** — https://repository.ub.edu.bi

ResearchGate

See discussions, stats, and author profiles for this publication at: https://www.researchgate.net/publication/267433916

Two-Aircraft Dynamic System on Approach. Flight Path and noise Optimization

Article · January 2012

CITATIONS
3

READS
137

3 authors:



Fulgence Nahayo
University of Burundi
17 PUBLICATIONS **36** CITATIONS
SEE PROFILE



Salah Khardi
Institut National des Sciences Appliquées de Lyon
74 PUBLICATIONS **721** CITATIONS
SEE PROFILE



Mounir Haddou
Institut National des Sciences Appliquées de Rennes
64 PUBLICATIONS **783** CITATIONS
SEE PROFILE

All content following this page was uploaded by Mounir Haddou on 17 December 2014.

The user has requested enhancement of the downloaded file.

Applied Mathematical Sciences, Vol. 6, 2012, no. 78, 3861 - 3880

Two-Aircraft Dynamic System on Approach. Flight Path and Noise Optimization

F. Nahayo[1,2], S. Khardi[1] and M. Haddou[3]

[1] IFSTTAR-LTE, The French Institute of Science and Technology for Transport, Development and Networks-Transport and Environment Laboratory, Lyon - France
nahayo.fulgence@gmail.com and salah.khardi@ifsttar.fr

[2] University Claude Bernard of Lyon 1, France
University of Burundi, Burundi

[3] INSA-IRMAR, UMR-CNRS 6625, Rennes - France

Abstract

The aim of this paper is to present and to solve a mathematical model of two-aircraft optimal control problem reducing noise during the approach. This is a non-convex optimal control problem governed by ordinary non-linear differential equations. A Symplectic Partitioned Runge-Kutta discretization and the Pontryaguin maximum principle are used. Discretization scheme provides a sufficiently high order requiring a computation of the partial derivatives of the aircraft dynamic parameters. The nonlinear interior point trust region optimization solver is applied. Numerical experiments and results are presented. They confirm the feasible optimized trajectories contributing to a significant noise reduction.

Keywords: Symplectic Partitioned Runge-Kutta algorithm, optimal control problem, AMPL programming, KNITRO, aircraft noise

1 Introduction

Aircraft noise levels have been studied in several papers [1, 2] . In this work, a theoretical model of noise optimization is developed while maintaining a reliable evolution of the flight procedures of two commercial aircraft on approach. In particular, this work is focused on aircraft coupling noise levels and energetic consumption. These two-aircraft are supposed to land successively on one runway without conflict [3]. It is all about the evolution of flight dynamics

and minimization of noise for two similar commercial landing aircraft taking into account the flight constraints. The model considered here is non-convex and non-linear optimal control problem leading to a system of non-linear ordinary differential equations [4]. In this model, the displacement of the two planes is described by a three dimensional set of non-linear ordinary differential equations subjected to state and control constraints. The functional to be minimized is an integral which describes the overall levels of noise collected on the ground, emitted by the two mentioned aircraft. The formulation of the problem takes into account several kinds of constraints such as aircraft stability, performance and flight safety. A Symplectic Partitioned Runge-Kutta method is used to transform the obtained set of non-linear ordinary differential equations to a set of non-linear algebric ones [5]. A commercial code namely The Nonlinear Interior point Trust Region Optimization solver 'KNITRO'[6] is used to solve the obtained algebraic non-linear system of equation implemented by A Modeling Language for Mathematical Programming 'AMPL' [7, 8]. The two-aircraft flight dynamic, the noise levels, the constraints, the mathematical basic equations of the two-aircraft acoustic optimal control problem and the Symplectic Partitioned Runge-Kutta discretization scheme are presented in sections 2 and 3 while the numerical experiments are presented in the last section.

2 Mathematical description of the OC problem

The three dimensional motion of each aircraft $A_i, i \in \{1, 2\}$ where i stands for the first and second aircraft respectively , is described in three frames, namely landmark $R_O(O, \overrightarrow{X}_1, \overrightarrow{Y}_1, \overrightarrow{Z}_1)$, aircraft frame $R_b(G_i, \overrightarrow{X}_{Gi}, \overrightarrow{Y}_{Gi}, \overrightarrow{Z}_{Gi})$ and aerodynamic frame $R_a(G_i, \overrightarrow{X}_{ai}, \overrightarrow{Y}_{ai}, \overrightarrow{Z}_{ai})$ [9]. The transfer matrices connecting these frames are given in [10]. The equations of motion of each aircraft read:

$$\begin{array}{ll} \sum \overrightarrow{F}_{ext_i} - \frac{dm_i}{dt}\overrightarrow{V_{a_i}} & = \frac{m_i d\overrightarrow{V}_{a_i}}{dt} \\ \sum \overrightarrow{M}_{ext_{G_i}} & = \frac{d}{dt}[I_{G_i}\overrightarrow{\Omega}_i] \end{array} \tag{1}$$

The index i = 1, 2 stands for the first and second aircraft. In the above system, $\overrightarrow{F}_{ext_i}$ represents the external forces acting on the aircraft, $m_i(t)$ the mass of the aircraft, V_{ai} the airspeed of aircraft, $\overrightarrow{M}_{ext_{G_i}}$ the external moments of each aircraft, $I(G_i, A_i)$ the inertia matrix. The time derivation is for an observer attached to frame R_O and the equations are written in R_a. The acceleration is obtained with two time derivations of the position. The relations between the derivatives in the two frames are connected by the following equation:

$$\frac{d\overrightarrow{X}}{dt}|_{R_O} = \frac{d\overrightarrow{X}}{dt}_{R_a} + \overrightarrow{\Omega}_{R_a/R_O} \times \overrightarrow{X}$$

where $\frac{d\overrightarrow{X}}{dt}|_{R_O}$ is the derivative with respect to time of the vector $\overrightarrow{X}$ in the vehicle-carried normal Earth frame R_O, $\frac{d\overrightarrow{X}}{dt}|_{R_a}$ is the derivative with respect to time of the vector $\overrightarrow{X}$ in the frame R_a , Ω_i is the angular velocity of the aircraft and $\overrightarrow{\Omega}_{R_a/R_O}$ is the angular velocity of the frame R_1 relative to the frame R_0. After transformations and simplifications, the system takes the following explicit form:

$$\begin{cases}
\dot{m}_i & = -C_{SR_i}P_0\delta_{xi}\frac{\rho_i}{\rho_0}(1-M_i+\frac{M_i^2}{2}) \\
\dot{V}_{a_i} & = \frac{1}{m_i}[-m_i g sin\gamma_{a_i} - \frac{1}{2}\rho_i S V_{a_i}^2 C_{D_i} \\
& +(cos\alpha_{a_i}cos\beta_{a_i} + sin\beta_{a_i} + sin\alpha_{a_i}cos\beta_{a_i})F_{x_i} \\
& +C_{SR_i}P_0\delta_{xi}\frac{\rho_i}{\rho_0}(1-M_i+\frac{M_i^2}{2})u_i - m_i\Delta A_u^i] \\
\dot{\beta}_{a_i} & = \frac{1}{m_i V_{a_i}}[m_i g cos\gamma_{a_i} sin\mu_{a_i} + \frac{1}{2}\rho_i S V_{a_i}^2 C_{y_i} \\
& +[-cos\alpha_{a_i}sin\beta_{a_i} + cos\beta_{a_i} - sin\alpha_{a_i}sin\beta_{a_i}]F_{y_i} \\
& +C_{SR_i}P_0\delta_{xi}\frac{\rho_i}{\rho_0}(1-M_i+\frac{M_i^2}{2})v_i - m_i\Delta A_v^i] \\
\dot{\alpha}_{a_i} & = \frac{1}{m_i V_{a_i} cos\beta_{a_i}}[m_i g cos\gamma_{a_i} cos\mu_{a_i} - \frac{1}{2}\rho_i S V_{a_i}^2 C_{L_i} \\
& +[-sin\alpha_{a_i} + cos\alpha_{a_i}]F_{z_i} \\
& +C_{SR_i}P_0\delta_{xi}\frac{\rho_i}{\rho_0}(1-M_i+\frac{M_i^2}{2})w_i - m_i\Delta A_w^i] \\
\dot{p}_i & = \frac{C}{AC-E^2}\{r_i q_i(B-C) - Ep_i q_i + \frac{1}{2}\rho_i S l V_{a_i}^2 C_{l_i} \\
& +\sum_{j=1}^{2} F_j[y_{M_{ij}}^b cos\beta_{m_{ij}} sin\alpha_{m_{ij}} - z_{M_{ij}}^b sin\beta_{m_{ij}}]\} \\
& +\frac{E}{AC-E^2}\{p_i q_i(A-B) - Er_i q_i + \frac{1}{2}\rho_i S l V_{a_i}^2 C_{ni} \\
& +\sum_{j=1}^{2} F_j[x_{M_{ij}}^b sin\beta_{m_{ij}} - y_{M_{ij}}^b cos\beta_{m_{ij}} cos\alpha_{m_{ij}}]\} \\
\dot{q}_i & = \frac{1}{B}\{-r_i p_i(A-C) - E(p_i^2 - r_i^2) + \frac{1}{2}\rho_i S l V_{a_i}^2 C_{mi} \\
& +\sum_{j=1}^{2} F_j[z_{M_{ij}}^b cos\beta_{m_{ij}} cos\alpha_{m_{ij}} - x_{M_{ij}}^b cos\beta_{m_{ij}} sin\alpha_{m_{ij}}]\} \\
\dot{r}_i & = \frac{E}{AC-E^2}\{r_i q_i(B-C) + Ep_i q_i + \frac{1}{2}\rho_i S l V_{a_i}^2 C_{l_i} \\
& +\sum_{j=1}^{2} F_j[y_{M_{ij}}^b cos\beta_{m_{ij}} sin\alpha_{m_{ij}} - z_{M_{ij}}^b sin\beta_{m_{ij}}]\} \\
& +\frac{A}{AC-E^2}\{p_i q_i(A-B) - Er_i q_i + \frac{1}{2}\rho_i S l V_{a_i}^2 C_{ni} \\
& +\sum_{j=1}^{2} F_j[x_{M_{ij}}^b sin\beta_{m_{ij}} - y_{M_{ij}}^b cos\beta_{m_{ij}} cos\alpha_{m_{ij}}]\} \\
\dot{X}_{G_i} & = V_{a_i} cos\gamma_{a_i} cos\chi_{a_i} + u_w \\
\dot{Y}_{G_i} & = V_{a_i} cos\gamma_{a_i} sin\chi_{a_i} + v_w \\
\dot{Z}_{G_i} & = -V_{a_i} sin\gamma_{a_i} + w_w \\
\dot{\phi}_i & = p_i + q_i sin\phi_i tan\theta_i + r_i cos\phi_i tan\theta_i \\
\dot{\theta}_i & = q_i cos\phi_i - r_i sin\phi_i \\
\dot{\psi}_i & = \frac{sin\phi_i}{cos\theta_i}q_i + \frac{cos\phi_i}{cos\theta_i}r_i
\end{cases} \tag{2}$$

where $j \in \{1,2\}$ stands for the first and second engine of each aircraft i, the expressions $A = I_{xx}, B = I_{yy}, C = I_{zz}, E = I_{xz}$ are the inertia moments of the aircraft, ρ_i is the air density, S is the aircraft reference area, l is the aircraft reference length, g is the acceleration due to gravity,

$$C_{D_i} = C_{D0} + kC_{Li}^2$$

is the drag coefficient,

$$C_{yi} = C_{y\beta}\beta + C_{yp}\frac{pl}{V} + C_{yr}\frac{rl}{V} + C_{Y\delta_l}\delta_{li} + C_{Y\delta_n}\delta_{ni}$$

is the lateral forces coefficient,

$$C_{Li} = C_{L\alpha}(\alpha_a - \alpha_{a0}) + C_{L\delta_m}\delta_{mi} + C_{LM}M_i + C_{Lq}\frac{q_a^b l}{V}$$

is the lift coefficient,

$$C_{li} = C_{l\beta}\beta + C_{lp}\frac{pl}{V} + C_{lr}\frac{rl}{V} + C_{l\delta_l}\delta_{li} + C_{l\delta_n}\delta_{ni}$$

is the rolling moment coefficient,

$$C_{mi} = C_{m0} + C_{m\alpha}(\alpha - \alpha_0) + C_{m\delta_m}\delta_{mi}$$

is the pitching moment coefficient,

$$C_{ni} = C_{n\beta}\beta + C_{np}\frac{pl}{V} + C_{nr}\frac{rl}{V} + C_{n\delta_l}\delta_{li} + C_{n\delta_n}\delta_{ni}$$

is the yawing moment coefficient, $(x^b_{Mij}, x^b_{Mij}, x^b_{Mij})$ is the position of the engine in the body frame, P_0 is the full thrust, ρ_0 is the atmospheric density at the ground, $F = (F_{xi}, F_{yi}, F_{zi})$ is the propulsive force, $V_{ai} = (u_i, v_i, w_i)$ is the aerodynamic speed, $(\Delta A^i_u, \Delta A^i_v, \Delta A^i_w)$ is the complementary acceleration, (u_w, v_w, w_w) is the wind velocity, β_{mij} is the yaw setting of the engine and α_{mij} is the pitch setting of the engine. The mass change is reflected in the aircraft fuel consumption as described by Torenbeek [11] where the specific consumption is:

$$C_{SR_i} = 2.01 \times 10^{-5}\frac{(\Phi - \mu_i - \frac{K_i}{\eta_c})\sqrt{\Theta}}{\sqrt{5\eta_n(1+\eta_{tf_i}\lambda)}\sqrt{G_i + 0.2M_i^2\frac{\eta_{d_i}}{\eta_{tf_i}}\lambda} - (1-\lambda)M_i}$$

with the generating function G_i:

$$\begin{aligned} G &= (\Phi - \tfrac{K_i}{\eta_c})(1 - \tfrac{1.01}{\eta_i^{\frac{\nu-1}{\nu}}(K_i+\mu_i)(1-\frac{K_i}{\Phi\eta_c\eta_t})}) \\ K_i &= \mu_i(\epsilon_c^{\frac{\nu-1}{\nu}} - 1) \\ \mu_i &= 1 + \tfrac{\nu-1}{2}M_i^2 \end{aligned}$$

The nomenclature of engine performance variables are given by G_i the gas generator power function, G0 the gas generator power function (static, sea level), K the temperature function of compression process, M_i the flight Mach number, T4 the turbine Entry total Temperature, T0 the ambient temperature

at sea level, T the flight temperature, while the nomenclature of engines yields is $\eta_c = 0.85$ the isentropic compressor efficiency:

$$\eta_{d_i} = 1 - 1.3(\frac{0.05}{Re^{\frac{1}{5}}})^2(\frac{0.5}{M_i})^2\frac{L}{D}$$

the isentropic fan intake duct efficiency, L the duct length, D the inlet diameter, Re the Reynolds number at the entrance of the nozzle:

$$\eta_{f_i} = 0.86 - 3.13 \times 10^{-2} M_i$$

the isentropic fan efficiency:

$$\eta_i = \frac{1 + \eta_{d_i}\frac{\gamma-1}{2}M_i^2}{1 + \frac{\gamma-1}{2}M_i^2}$$

the gas generator intake stagnation pressure ratio, $\eta_n = 0.97$ the isentropic efficiency of expansion process in nozzle, $\eta_t = 0.88$ the isentropic turbine efficiency $\eta_{tf_i} = \eta_t\eta_{f_i}$, ϵ_c the overall pressure ratio (compressor), ν the ratio of specific heats $\nu = 1.4$, λ the bypass ratio, μ_i the ratio of stagnation to static temperature of ambient air, Φ the nondimensional turbine entry temperature $\Phi = \frac{T_4}{T}$ and Θ the relative ambient temperature $\Theta = \frac{T}{T_0}$. The expressions $\alpha_{ai}(t), \beta_{ai}(t), \theta_i(t), \psi_i(t), \phi_i(t), V_{a_i}(t), X_{G_i}(t), Y_{G_i}(t), Z_{G_i}(t), p_i(t), q_i(t), r_i(t), m_i(t)$ are respectively the attack angle, the aerodynamic sideslip angle, the inclination angle, the cup, the roll angle, the airspeed, the position vectors, the roll velocity of the aircraft relative to the earth, the pitch velocity of the aircraft relative to the earth, the yaw velocity of the aircraft relative to the earth and the aircraft mass.

The system (2) could be written in a simplified form:

$$\frac{d\mathbf{y}_i(t)}{dt} = \mathbf{f}_i(\mathbf{y}_i(t), \mathbf{u}_i(t)) \tag{3}$$

henceforth $\mathbf{y}_i$ is called a state function:

$$\begin{array}{l}\mathbf{y}_i : [t_0, t_f] \longrightarrow \mathbf{R^{13}} \\ \mathbf{y}_i(t) = (\alpha_{ai}(t), \beta_{ai}(t), \theta_{ai}(t), \psi_{ai}(t), \phi_i(t), V_{a_i}(t), X_{G_i}(t), Y_{G_i}(t), Z_{G_i}(t), p_i(t) \\ q_i(t), r_i(t), m_i(t))\end{array} \tag{4}$$

The control vector is:

$$\begin{array}{rl}\mathbf{u}_i : [t_0, t_f] & \longrightarrow \mathbf{R^4} \\ t & \longrightarrow \mathbf{u}_i(t) = (\delta_{l_i}(t), \delta_{m_i(t)}, \delta_{n_i}(t), \delta_{x_i}(t))\end{array} \tag{5}$$

where the expressions $\delta_{l_i}(t), \delta_{m_i(t)}, \delta_{n_i}(t), \delta_{x_i}(t)$ are respectively the roll control, the pitch control, the yaw control and the thrust control. The dynamics relationship can be written as:

$$\dot{\mathbf{y}}_i(t) = \mathbf{f}_i(\mathbf{y}_i, \mathbf{u}_i, t), \forall t \in [0, T], y_i(0) = y_{i0} \tag{6}$$

The angles $\gamma_{a_i}(t), \chi_{a_i}(t), \mu_{a_i}(t)$ corresponding respectively to the aerodynamic climb angle (air-path inclination angle), the aerodynamic azimuth (air-path track angle) and the air-path bank angle (aerodynamic bank angle) are not taken as state in this model. To simplify the model, the atmosphere standards conditions are considered. The engine angles, the complementary acceleration and the aerodynamic sideslip angle are neglected because the wind is constant and there is no engine failure. With some complex mathematical transformations, the dynamic system (2) becomes:

$$\begin{cases}
\dot{m}_i & = -C_{SR_i} P_0 \delta_{xi} \frac{\rho_i}{\rho_0}(1 - M_i + \frac{M_i^2}{2}) \\
\dot{V_{a_i}} & = \frac{1}{m_i}[-m_i g sin\gamma_{a_i} - \frac{1}{2}\rho_i S V_{a_i}^2 C_{D_i} \\
& +(cos\alpha_{a_i} + sin\alpha_{a_i})F_{x_i} + C_{SR_i} P_0 \delta_{xi} \frac{\rho_i}{\rho_0}(1 - M_i + \frac{M_i^2}{2})u_i] \\
\dot{\alpha_{a_i}} & = \frac{1}{m_i V_{a_i} cos\beta_{a_i}}[m_i g cos\gamma_{a_i} cos\mu_{a_i} - \frac{1}{2}\rho_i S V_{a_i}^2 C_{L_i} \\
& +[cos\alpha_{a_i} - sin\alpha_{a_i}]F_{z_i} + C_{SR_i} P_0 \delta_{xi} \frac{\rho_i}{\rho_0}(1 - M_i + \frac{M_i^2}{2})w_i] \\
\dot{p}_i & = \frac{C}{AC - E^2}\{r_i q_i (B - C) - E p_i q_i + \frac{1}{2}\rho_i S l V_{a_i}^2 C_{l_i}\} \\
& +\frac{E}{AC - E^2}\{p_i q_i (A - B) - E r_i q_i + \frac{1}{2}\rho S l V_{a_i}^2 C_{ni} \\
\dot{q}_i & = \frac{1}{B}\{-r_i p_i (A - C) - E(p_i^2 - r_i^2) + \frac{1}{2}\rho_i S l V_{a_i}^2 C_{mi}\} \\
\dot{r}_i & = \frac{E}{AC - E^2}\{r_i q_i (B - C) + E p_i q_i + \frac{1}{2}\rho_i S l V_{a_i}^2 C_{l_i} \\
& +\frac{A}{AC - E^2}\{p_i q_i (A - B) - E r_i q_i + \frac{1}{2}\rho_i S l V_{a_i}^2 C_{ni}\} \\
\dot{X}_{G_i} & = V_{a_i} cos\gamma_{a_i} cos\chi_{a_i} \\
\dot{Y}_{G_i} & = V_{a_i} cos\gamma_{a_i} sin\chi_{a_i} \\
\dot{Z}_{G_i} & = -V_{a_i} sin\gamma_{a_i} \\
\dot{\phi}_i & = p_i + q_i sin\phi_i tan\theta_i + r_i cos\phi_i tan\theta_i \\
\dot{\theta}_i & = q_i cos\phi_i - r_i sin\phi_i \\
\dot{\psi}_i & = \frac{sin\phi_i}{cos\theta_i} q_i + \frac{cos\phi_i}{cos\theta_i} r_i
\end{cases} \tag{7}$$

By the combination of this system with the aircraft control, one has the two-aircraft dynamic flight model as shown in (6). So, the state vector becomes:

$$\begin{aligned}
&\mathbf{y}_i : [t_0, t_f] \longrightarrow \mathbf{R^{12}} \\
&\mathbf{y}_i = (\alpha_{ai}(t), \theta_{ai}(t), \psi_{ai}(t), \phi_{ai}(t), V_{a_i}(t), X_{G_i}(t), Y_{G_i}(t), Z_{G_i}(t), p_i(t), q_i(t), r_i(t), m_i(t))
\end{aligned} \tag{8}$$

The previous state function together with the cost function and the set of constraints form the basic equations of the optimal control problem which shall be shown in the following paragraphs.

The objective function model. In this work, two different cost functions

are considered. In order to build the first cost function, let us define the quantity named The Sound Exposure Level 'SEL' [12, 13, 14]:

$$SEL = 10log\left[\int_{t'} 10^{0.1L_{A1,dt}(t)}dt\right] \tag{9}$$

where t' is the noise event interval. $[t_{10}, t_{1f}]$ and $[t_{20}, t_{2f}]$ are the respective approach intervals for the first and second aircraft, the objective function is calculated as:

$$\begin{aligned}
SEL_1 &= 10log\left[\tfrac{1}{t_o}\int_{t_{10}}^{t_{20}} 10^{0.1L_{A1,dt}(t)}dt\right], t \in [t_{10}, t_{20}] \\
SEL_{12} &= SEL_{11} \oplus SEL_{21} \\
&= 10\log[\tfrac{1}{t_o}\int_{t_{20}}^{t_{1f}} 10^{0.1L_{A1,dt}(t)}dt + \tfrac{1}{t_o}\int_{t_{20}}^{t_{1f}} 10^{0.1L_{A2,dt}(t)}dt], t \in [t_{20}, t_{1f}] \\
SEL_2 &= 10\log\left[\tfrac{1}{t_o}\int_{t_{1f}}^{t_{2f}} 10^{0.1L_{A2,dt}(t)}dt\right], t \in [t_{1f}, t_{2f}]
\end{aligned}$$

and finally, the first cost function reads:

$$\begin{aligned}
SEL_G &= \tfrac{(t_{20}-t_{10})SEL_1 \oplus (t_{1f}-t_{20})SEL_{12} \oplus (t_{2f}-t_{1f})SEL_2}{t_{2f}-t_{10}} \\
&= 10\log\{\tfrac{1}{t_{2f}-t_{10}}[(t_{20}-t_{10})\int_{t_{10}}^{t_{20}} 10^{0.1L_{A1}(t)}dt \\
&+(t_{1f}-t_{20})\int_{t_{20}}^{t_{1f}} 10^{0.1L_{A1}(t)}dt + (t_{1f}-t_{20})\int_{t_{20}}^{t_{1f}} 10^{0.1L_{A2}(t)}dt \\
&+(t_{2f}-t_{1f})\int_{t_{1f}}^{t_{2f}} 10^{0.1L_{A2}(t)}dt,]\}, t \in [t_{10}, t_{2f}]
\end{aligned} \tag{10}$$

where SEL_G is the cumulated two-aircraft noise and the operator $\oplus$ means the acoustic adding. Expressions $L_{A1}(t), L_{A2}(t)$ are equivalent and reflect the aircraft jet noise given by the formula [12, 15]:

$$\begin{aligned}
L_{A1}(t) = \; & 141 + 10\log\left(\frac{\rho_1}{\rho_i}\right)^w + 10\log\left(\frac{V_e}{c}\right)^{7.5} + 3\log\left(\frac{2s_1}{\pi d_1^2} + 0.5\right) \\
& +5\log\frac{\tau_1}{\tau_2} + 10\log\left[\left(1-\frac{v_2}{v_1}\right)^{me} + 1.2\frac{\left(1+\frac{s_2v_2^2}{s_1v_1^2}\right)^4}{\left(1+\frac{s_2}{s_1}\right)^3}\right] \\
& +10\log s_1 - 20\log R + \Delta V + 10\log\left[\left(\frac{\rho_i}{\rho_{ISA}}\right)^2\left(\frac{c}{c_{ISA}}\right)^4\right]
\end{aligned}$$

where v_1 is the jet speed at the entrance of the nozzle, v_2 the jet speed at the nozzle exit, τ_1 the inlet temperature of the nozzle, τ_2 the temperature at the nozzle exit, ρ_i the density of air, ρ_1 the atmospheric density at the entrance of the nozzle, ρ_{ISA} the atmospheric density at ground, s_1 the entrance area of the nozzle hydraulic engine: s_2 the emitting surface of the nozzle hydraulic engine, d_1 the inlet diameter of the nozzle hydraulic engine,

$$V_e = v_1[1 - (V/v_1)\cos(\alpha_p)]^{2/3}$$

the effective speed (α_p is the angle between the axis of the motor and the axis of the aircraft), R the source observer distance, w the exponent variable defined by:

$$w = \frac{3(V_e/c)^{3.5}}{0.6 + (V_e/c)^{3.5}} - 1$$

c the sound velocity (m/s), me the exhibiting variable depending on the type of aircraft:

$$me = 1.1\sqrt{\frac{s_2}{s_1}}, \quad \frac{s_2}{s_1} < 29.7; me = 6.0, \quad \frac{s_2}{s_1} \geq 29.7$$

the term:

$$\Delta V = -15log(C_D(M_c, \theta)) - 10log(1 - Mcos\theta),$$

means the Doppler convection when:

$$C_D(M_c, \theta) = [(1 + M_c cos\theta)^2 + 0.04M_c^2]$$

M the aircraft Mach Number, M_c the convection Mach Number:

$$M_c = 0.62(v_1 - Vcos(\alpha_p))/c$$

θ is the Beam angle. The objective formula above could be written in the following simplified form

$$J_{G12}(\mathbf{y}(.), \mathbf{u}(.)) = \int_{t'} g(\mathbf{y}(t), \mathbf{u}(t))dt$$

In the second case where the second plane is delayed δ_t from the first one, the flight procedures remain the same for the two-aircraft and the cost function is:

$$\begin{array}{ll} J(\mathbf{y}(.), \mathbf{u}(.)) & = \int_{t_0}^{t_0+\delta_t} 10^{0.1L_{A1}(t)}dt, t \in [t_0, t_0 + \delta_t] \\ J(\mathbf{y}(.), \mathbf{u}(.)) & = \int_{t_0+\delta_t}^{t_f} [10^{0.1L_{A1}(t)} + 10^{0.1L_{A2}(t-\delta_t)}]dt, t \in [t_0 + \delta_t, t_f] \\ J(\mathbf{y}(.), \mathbf{u}(.)) & = \int_{t_f}^{t_f+\delta_t} 10^{0.1L_{A2}(t-\delta_t)}dt, t \in [t_f, t_f + \delta_t] \end{array} \quad (11)$$

where $L_{A2}(t) = L_{A1}(t)$.

Constraints. The considered constraints concern aircraft flight speeds and altitudes, flight angles and control positions, energy, aircraft separation:

1. The vertical separation given by $Z_{G_{12}} = Z_{G_2} - Z_{G_1}$ where Z_{G_1}, Z_{G_2} are respectively the altitude of the first and second aircraft and $Z_{G_{12}}$ the altitude separation.

2. The horizontal separation $X_{G_{12}} = X_{G_1} - X_{G_2}$ [16, **?**, 17] where X_{G_1}, X_{G_2} are horizontal positions of the first and second aircraft and their separation distance.

3. The aircraft speed V_{a_i} must be bounded as follows $1.3V_s \leq V_{a_i} \leq V_{if}$ where V_s is the stall speed,V_{if} is the maximum speed and $V_{io} = 1.3V_s$ the minimum speed of the aircraft A_i [19, 11], the roll velocity of the aircraft $p_i \in [p_{i0}, p_{if}]$, the pitch velocity of the aircraft $q_i \in [q_{i0}, q_{if}]$ and the yaw velocity of the aircraft $r_i \in [r_{i0}, r_{if}]$.

4. On the approach, the ICAO standards and aircraft manufacturers require flight angle evolution as follows: attack angle $\alpha_{a_i} \in [\alpha_{io}, \alpha_{if}]$, the inclination angle $\theta_i \in [\theta_{i0}, \theta_{if}]$ and the roll angle $\phi_i \in [\phi_{io}, \phi_{if}]$.

5. The aircraft control $\delta(t) = (\delta_{l_i}(t), \delta_{m_i(t)}, \delta_{n_i}(t), \delta_{x_i}(t))$ is maintained between the position δ_{li0} and δ_{lif} for the roll control, δ_{mi0} and δ_{mif} for the pitch control, δ_{ni0} and δ_{nif} for the yaw control and δ_{xi0} and δ_{xif} for the thrust.

6. The mass m_i of the aircraft A_i is variable: $m_{i0} < m_i < m_{if}, i = 1, 2$. This constraint results in energy consumption of the aircraft [20, 21].

On the whole, the constraints come together under the relationship:

$$\begin{array}{l} \mathbf{k}_{1i}(\mathbf{y}_i, \mathbf{u}_i) \leq 0 \\ \mathbf{k}_{2i}(\mathbf{y}_i, \mathbf{u}_i) \geq 0 \end{array} \tag{12}$$

where

$$\begin{array}{l} \mathbf{k}(t) : \mathbf{R^{12}} \times \mathbf{R^4} \longrightarrow \mathbf{R^{16}}, (\mathbf{y}_i, \mathbf{u}_i) \longrightarrow k_i(\mathbf{y}_i, \mathbf{u}_i) \\ \mathbf{k}_{1i}(\mathbf{y}_i, \mathbf{u}_i) = (\alpha_i(t) - \alpha_{if}, \theta_i(t) - \theta_{if}, \psi_i(t) - \psi_{if}, \phi_i(t) - \phi_{if}, V_{a_i}(t) - V_{aif} \\ \qquad X_{G_i}(t) - X_{Gif}, Y_{G_i}(t) - Y_{Gif}, Z_{G_i}(t) - Z_{Gif}, p_i(t) - p_{if}, q_i(t) - q_{if} \\ \qquad r_i(t) - r_{if}, \delta_{l_i}(t) - \delta_{l_if}, \delta_{m_i}(t) - \delta_{mif}, \delta_{n_i}(t) - \delta_{nif}, \delta_{x_i}(t) - \delta_{xif} \\ \qquad m_i(t) - m_{if}) \\ k_{2i}(\mathbf{y}_i, \mathbf{u}_i) = (\alpha_i(t) - \alpha_{i0}, \theta_i(t) - \theta_{i0}, \psi_i(t) - \psi_{i0}, \phi_i(t) - \phi_{i0}, V_{a_i}(t) - V_{ai0} \\ \qquad X_{G_i}(t) - X_{Gi0}, Y_{G_i}(t) - Y_{Gi0}, Z_{G_i}(t) - Z_{Gi0}, p_i(t) - p_{i0}, q_i(t) - q_{i0} \\ \qquad r_i(t) - r_{i0}, \delta_{l_i}(t) - \delta_{l_i0}, \delta_{m_i}(t) - \delta_{mi0}, \delta_{n_i}(t) - \delta_{ni0}, \delta_{x_i}(t) - \delta_{xi0} \\ \qquad m_i(t) - m_{i0}). \end{array}$$

The following values reflect the digital applications considered for the two-aircraft [10, 11, 12, 20].

Table: Limit values for the two-aircraft in approach	
maximum value	minimum value
$V_{a1f} = V_{a2f} = 200\ m/s$	$V_{a10} = V_{a20} = 73.45\ m/s$
$Z_{G1f} = 35 \times 10^2\ m$	$Z_{G10} = 0\ m$
$Z_{G2f} = 41 \times 10^2\ m$	$Z_{G20} = 0\ m$
$\delta_{l1f} = \delta_{l2f} = 0.0174$	$\delta_{l10} = \delta_{l20} = -0.0174$
$\delta_{m1f} = \delta_{m2f} = 0.087$	$\delta_{m10} = \delta_{m20} = 0$
$\delta_{n1f} = \delta_{n2f} = 0.314$	$\delta_{n10} = \delta_{n20} = -0.035$
$\delta_{x1f} = \delta_{x2f} = 0.6$	$\delta_{x10} = \delta_{x20} = 0.2$
$\alpha_{a1f} = \alpha_{a2f} = 20^\circ$	$\alpha_{a10} = \alpha_{a20} = 2^\circ$
$\theta_{a1f} = \theta_{a2f} = 7^\circ$	$\theta_{a10} = \theta_{a20} = -7^\circ$
$\gamma_{a1f} = \gamma_{a2f} = 0^\circ$	$\gamma_{a10} = \gamma_{a20} = -5^\circ$
$\mu_{a1f} = \mu_{a2f} = 3^\circ$	$\mu_{a10} = \mu_{a20} = -2^\circ$
$\chi_{a1f} = \chi_{a2f} = 5^\circ$	$\chi_{a10} = \chi_{a20} = -5^\circ$
$\phi_{a1f} = \phi_{a2f} = 1^\circ$	$\phi_{a10} = \phi_{a20} = -1^\circ$
$\psi_{a1f} = \psi_{a2f} = 3^\circ$	$\psi_{a10} = \psi_{a20} = -3^\circ$
$t_{1f} = 300\ s$,$t_{2f} = 390\ s$	$t_{10} = 0\ s$, $t_{20} = 90\ s$
$m_{10} \simeq 1.1 \times 10^5\ kg$,	$m_{1f} \simeq 1.09055 \times 10^5\ kg$,
$m_{20} \simeq 1.10071 \times 10^5\ kg$	$m_{2f} \simeq 1.09126 \times 10^5\ kg$
$A = 5.555 \times 10^6\ kg\ m^2$	$B = 9.72 \times 10^6\ kg\ m^2$
$C = 14.51 \times 10^6\ kg\ m^2$	$E = -3.3 \times 10^4\ kg\ m^2$
$Z_{12} = 2 \times 10^3\ ft \simeq 6 \times 10^2\ m$	
$X_{G_{12}} = 5\ NM \simeq 9 \times 10^3\ m$	
$p_{1f} = p_{2f} = 1^\circ s^{-1}$	$p_{10} = p_{20} = -1^\circ s^{-1}$
$q_{1f} = q_{2f} = 3.6^\circ s^{-1}$	$q_{10} = q_{20} = 3^\circ s^{-1}$
$r_{1f} = r_{2f} = 12^\circ s^{-1}$	$r_{10} = r_{20} = -12^\circ s^{-1}$

The two-aircraft acoustic optimal control problem. The combination of the aircraft dynamic equation (3) and (7), the aircraft objective function from equations (10) and the aircraft flight constraints (12), the two-aircraft acoustic optimal control problem is given as follows:

$$\begin{cases} \min_{u\in\mathbf{U}} J_{G12}(\mathbf{y}(.),\mathbf{u}(.)) = \int_{t10}^{t_{1f}} g_1(\mathbf{y}_1(t),\mathbf{u}_1(t),t)dt \\ + \int_{t20}^{t_{1f}} g_{12}(\mathbf{y}_1(t),\mathbf{u}_1(t),\mathbf{y}_2(t),\mathbf{u}_2(t),t)dt + \int_{t20}^{t_{2f}} g_2(\mathbf{y}_2(t),\mathbf{u}_2(t),t)dt + \phi(y(t_f)) \\ \dot{\mathbf{y}}(t) = \mathbf{f}(\mathbf{u}(t),\mathbf{y}(t)), \mathbf{u}(t) = (\mathbf{u}_1(t),\mathbf{u}_2(t)), \mathbf{y}(t) = (\mathbf{y}_1(t),\mathbf{y}_2(t)) \\ \forall t \in [t_{10}, t_{2f}], t_{10} = 0, \mathbf{y}(0) = \mathbf{y}_0, \mathbf{u}(0) = \mathbf{u}_0 \\ \mathbf{k}_{1i}(\mathbf{y}_i,\mathbf{u}_i) \leq 0 \\ \mathbf{k}_{2i}(\mathbf{y}_i,\mathbf{u}_i) \geq 0 \end{cases} \tag{13}$$

where g_{12} shows the aircraft coupling noise function and J_{G12} is the SEL of the two A300-aircraft.

3 Numerical processing

The problem as defined in the relation (13) is an optimal control problem [22, 23, 24] with instantaneous constraints:

$$\begin{cases} \min_{\mathbf{u}\in\mathbf{U}} J_{12}(\mathbf{y}(.),\mathbf{u}(.)) = \int_{t0}^{t_f} g(\mathbf{y}(t),\mathbf{u}(t))dt \\ \dot{\mathbf{y}}(t) = \mathbf{f}(\mathbf{y}(t),\mathbf{u}(t)) \\ \mathbf{k}_1(\mathbf{y},\mathbf{u},t) \leq 0 \\ \mathbf{k}_2(\mathbf{y},\mathbf{u},t) \geq 0 \end{cases} \tag{14}$$

where

$$\begin{aligned} \mathbf{k}_{1i}(\mathbf{y}_i,\mathbf{u}_i) = \; & (\alpha_i(t)-\alpha_{if}, \theta_i(t)-\theta_{if}, \psi_i(t)-\psi_{if}, \phi_i(t)-\phi_{if}, V_{a_i}(t)-V_{aif} \\ & X_{G_i}(t)-X_{Gif}, Y_{G_i}(t)-Y_{Gif}, Z_{G_i}(t)-Z_{Gif}, p_i(t)-p_{if} \\ & q_i(t)-q_{if}, r_i(t)-r_{if}, \delta_{l_i}(t)-\delta_{l_if}, \delta_{m_i}(t)-\delta_{mif}, \delta_{n_i}(t)-\delta_{nif} \\ & \delta_{x_i}(t)-\delta_{xif}, m_i(t)-m_{if}) \\ \mathbf{k}_{2i}(\mathbf{y}_i,\mathbf{u}_i) = \; & (\alpha_i(t)-\alpha_{i0}, \theta_i(t)-\theta_{i0}, \psi_i(t)-\psi_{i0}, \phi_i(t)-\phi_{i0}, V_{a_i}(t)-V_{ai0} \\ & X_{G_i}(t)-X_{Gi0}, Y_{G_i}(t)-Y_{Gi0}, Z_{G_i}(t)-Z_{Gi0}, p_i(t)-p_{i0} \\ & q_i(t)-q_{i0}, r_i(t)-r_{i0}, \delta_{l_i}(t)-\delta_{l_i0}, \delta_{m_i}(t)-\delta_{mi0}, \delta_{n_i}(t)-\delta_{ni0}, \\ & \delta_{x_i}(t)-\delta_{xi0}, m_i(t)-m_{i0}) \end{aligned} \tag{15}$$

Consider the pseudo-Hamiltonian of the system (15) given by:

$$H(\mathbf{y},\mathbf{u},\tilde{\mathbf{p}},\tilde{\mathbf{p}}_0,t) = \tilde{\mathbf{p}}^T\mathbf{F}(\mathbf{y},\mathbf{u},t) - \tilde{\mathbf{p}}_0 g(\mathbf{y},\mathbf{u},t) - \mu_1\mathbf{k}_1(\mathbf{y},\mathbf{u},t) - \mu_2\mathbf{k}_2(\mathbf{y},\mathbf{u},t) \tag{16}$$

where $\tilde{\mathbf{p}} = (\tilde{\mathbf{p}}_1, \tilde{\mathbf{p}}_2), \tilde{\mathbf{p}}_i = (\tilde{p}_{1i}, \tilde{p}_{2i}, \tilde{p}_{3i}, \tilde{p}_{4i}, \tilde{p}_{5i}, \tilde{p}_{6i}, \tilde{p}_{7i}, \tilde{p}_{8i}, \tilde{p}_{9i}, \tilde{p}_{10i}, \tilde{p}_{11i}, \tilde{p}_{12i}, \tilde{p}_{13i})^T$ is the adjoint state. With this new Pontryagin formulation, optimality necessary conditions are given by:

$$\begin{aligned} & H_{\mathbf{u}}(\mathbf{y},\mathbf{u},\tilde{\mathbf{p}},\tilde{\mathbf{p}}_0,t) = 0 \\ & \dot{\mathbf{y}} = H_{\tilde{\mathbf{p}}}(\mathbf{y},\mathbf{u},\tilde{\mathbf{p}},\tilde{\mathbf{p}}_0,t) = \mathbf{F}(\mathbf{y}(t),\mathbf{u}(t)) \\ & \dot{\tilde{\mathbf{p}}} = -H_{\mathbf{y}}(\mathbf{y},\mathbf{u},\tilde{\mathbf{p}},\tilde{\mathbf{p}}_0,t) \\ & \mathbf{k}_1(\mathbf{y},\mathbf{u},t) \leq 0, \mathbf{k}_2(\mathbf{y},\mathbf{u},t) \geq 0, t \in [t_0,t_f], \mu_2 \geq 0 \end{aligned} \tag{17}$$

where H a pseudo-hamiltonian. From equation $H_{\mathbf{u}}(\mathbf{y},\mathbf{u},\tilde{\mathbf{p}},\tilde{\mathbf{p}}_0,t) = 0$,with some regularity assumptions, one has:

$$\mathbf{u}(t) = \psi(\mathbf{y}(t),\tilde{\mathbf{p}}(t)) \tag{18}$$

The Hamiltonian is then:

$$\mathcal{H}(\mathbf{y},\mathbf{u},\tilde{\mathbf{p}},\tilde{\mathbf{p}}_0,t) = H(\psi(\mathbf{y},\tilde{\mathbf{p}}),\mathbf{y},\tilde{\mathbf{p}}) \tag{19}$$

The Hamilton system becomes:

$$\begin{aligned} & \dot{\mathbf{y}} = \mathcal{H}_{\tilde{\mathbf{p}}}(\mathbf{y},\mathbf{u},\tilde{\mathbf{p}},\tilde{\mathbf{p}}_0,t), \mathbf{y}(t_0) = \mathbf{y}_0 \\ & \dot{\mathbf{p}} = -\mathcal{H}_{\mathbf{y}}(\mathbf{y},\mathbf{u},\tilde{\mathbf{p}},\tilde{\mathbf{p}}_0,t), \tilde{\mathbf{p}}(t_f) = \phi'(\mathbf{y}(t_f)) \\ & \mathbf{k}_1(\mathbf{y},\mathbf{u},t) \leq 0, \mathbf{k}_2(\mathbf{y},\mathbf{u},t) \geq 0, t \in [t_0,t_f] \end{aligned} \tag{20}$$

The above system is a Hamiltonian system. Conservation of the Hamiltonian can not be guaranteed along numerical solutions. $\mathbf{y}_n, \tilde{\mathbf{p}}_n, \mathbf{u}_{n_k}$ and $\mathbf{q}_{n_k}$ are considered as an optimal solution of the problem:

$$\begin{cases} \min\limits_{\mathbf{u}_{n_k}} J_{12}(\mathbf{y}_n, \mathbf{u}_{n_k}) \\ \mathbf{y}_{n+1} = \mathbf{y}_n + h\sum\limits_{k=1}^{s} b_k \mathbf{F}(\mathbf{y}_{n_k}, \mathbf{u}_{n_k}), \mathbf{y}(t_0) = \mathbf{y}_0 \\ \mathbf{y}_{n_k} = \mathbf{y}_n + h\sum\limits_{j=1}^{s} a_k j \mathbf{F}(\mathbf{y}_{n_j}, \mathbf{u}_{n_j}), k = 1, ..., s \\ \mathbf{k}_1(\mathbf{y}_n, \mathbf{u}_{n_k}) \leq 0 \\ \mathbf{k}_2(\mathbf{y}_n, \mathbf{u}_{n_k}) \geq 0 \end{cases}$$

when the following conditions are true:

$$\begin{array}{ll} L_{\mathbf{y}_n} & = \nabla_{\mathbf{y}_n}(L_n + L_{n+1}) = 0 \\ L_{\mathbf{y}_{n_k}} & = \nabla_{\mathbf{y}_{n_k}} L_{n+1} = 0, k = 1, ..., s \\ L_{\mathbf{u}_{n_k}} & = \nabla_{\mathbf{u}_{n_k}} L_{n+1} = 10, k = 1, ..., s \\ L_{\tilde{\mathbf{p}}_n} & = \nabla_{\tilde{\mathbf{p}}_n} L_n = 0, n = 0, ..., N \\ L_{\mathbf{q}_{n_k}} & = \nabla_{\mathbf{q}_{n_k}} L_{n+1} = 0, k = 1, ..., s \end{array} \tag{21}$$

The Lagrangian L is given by the formula:

$$\begin{array}{ll} L & = g(\mathbf{y}_n, \mathbf{u}_{n_k}) + L_0 + \sum\limits_{n=0}^{N-1} L_{n+1} \\ L_0 & = \tilde{\mathbf{p}}_0^T \left(\mathbf{y}_(t_0) - \mathbf{y}_0\right) \\ L_{n+1} & = \tilde{\mathbf{p}}_{n+1}^T \left(\mathbf{y}_n - \mathbf{y}_{n+1} + h\sum\limits_{j=1}^{s} b_j \mathbf{F}(\mathbf{u}_{n_j}, \mathbf{y}_{n_j})\right) \\ & \quad + \sum\limits_{k=1}^{s} \mathbf{q}_{n_k}^T \left(\mathbf{y}_n - \mathbf{y}_{n_k} + h\sum\limits_{j=1}^{s} a_{kj} \mathbf{F}(\mathbf{u}_{n_j}, \mathbf{y}_{n_j})\right) \forall n = 0, ..., N-1 \end{array} \tag{22}$$

Considering $M = (\overline{A}, b)$ and $\tilde{M} = (\tilde{A}, \tilde{b})$ where M is the matrix of coefficients in the state equation and $\tilde{M}$ the coefficients matrix in the co-state equation, application of a symplectic partitioned Runge-Kutta method leads to a system

:

$$
\begin{aligned}
&\mathbf{y}_{n+1} = \mathbf{y}_n + h\sum_{k=1}^{s} b_k \mathcal{H}_{\tilde{\mathbf{p}}}(\mathbf{u}_{n_k}, \mathbf{y}_{n_k}), \mathbf{y}(t_0) = \mathbf{y}_0 \\
&\mathbf{y}_{n_k} = \mathbf{y}_n + h\sum_{j=1}^{s} a_{kj} \mathcal{H}_{\tilde{\mathbf{p}}}(\mathbf{u}_{n_j}, \mathbf{y}_{n_j}), k = 1, .., s \\
&\tilde{\mathbf{p}}_{n+1} = \tilde{\mathbf{p}}_n - h\sum_{k=1}^{s} \tilde{b}_k \mathcal{H}_{\mathbf{y}}(\tilde{\mathbf{p}}_{n_k}, \mathbf{y}_{n_k}), \tilde{\mathbf{p}}_N = \phi'(t_f) \\
&\tilde{\mathbf{p}}_{n_k} = \tilde{\mathbf{p}}_n - h\sum_{j=1}^{s} \tilde{a}_{kj} \mathcal{H}_{\mathbf{y}}(\tilde{\mathbf{p}}_{n_j}, \mathbf{y}_{n_j}) \\
&\mathcal{H}(\mathbf{y}_{n_k}, \tilde{\mathbf{p}}_{n_k}) = H(\psi(\mathbf{y}_{n_k}, \tilde{\mathbf{p}}_{n_k}), \mathbf{y}_{n_k}, \tilde{\mathbf{p}}_{n_k}) \\
&\tilde{a}_{kj} := b_j - \frac{b_j}{b_k} a_{jk}, b_j = \tilde{b}_j \\
&\mathbf{k}_1(\mathbf{y}_n, \mathbf{u}_{n_k}) \leq 0 \\
&\mathbf{k}_2(\mathbf{y}_n, \mathbf{u}_{n_k}) \geq 0
\end{aligned}
\tag{23}
$$

Algorithm 1:

1. Let us subdivide the time interval $[t_0, t_f]$ as $h = t_{n+1} - t_n = \frac{t_f - t_0}{N}$, where N is the number of samples in numerical schema.

2. For $0 \leq n \leq N$, we obtained :

$$
\begin{aligned}
&H_{\mathbf{u}}(\mathbf{u}_{ki}, \mathbf{y}_{ki}, \tilde{\mathbf{p}}_{ki}) = 0 \\
&\mathbf{y}_{n+1} = \mathbf{y}_n + h\sum_{k=1}^{s} b_k \mathcal{H}_{\tilde{\mathbf{p}}}(\mathbf{u}_{n_k}, \mathbf{y}_{n_k}), \mathbf{y}(t_0) = \mathbf{y}_0 \\
&\mathbf{y}_{n_k} = \mathbf{y}_n + h\sum_{j=1}^{s} a_{kj} \mathcal{H}_{\tilde{\mathbf{p}}}(\mathbf{u}_{n_j}, \mathbf{y}_{n_j}), k = 1, .., s \\
&\tilde{\mathbf{p}}_{n+1} = \tilde{\mathbf{p}}_n - h\sum_{k=1}^{s} \tilde{b}_k \mathcal{H}_{\mathbf{y}}(\tilde{\mathbf{p}}_{n_k}, \mathbf{y}_{n_k}, \mathbf{u}_{n_k}), \tilde{\mathbf{p}}_N = \phi'(t_f) \\
&\tilde{\mathbf{p}}_{n_k} = \tilde{\mathbf{p}}_n - h\sum_{j=1}^{s} \tilde{a}_{kj} \mathcal{H}_{\mathbf{y}}(\tilde{\mathbf{p}}_{n_j}, \mathbf{y}_{n_j}, \mathbf{u}_{n_j}) \\
&\mathcal{H}(\mathbf{y}_{n_k}, \tilde{\mathbf{p}}_{n_k}) = H(\psi(\mathbf{y}_{n_k}, \tilde{\mathbf{p}}_{n_k}), \mathbf{y}_{n_k}, \tilde{\mathbf{p}}_{n_k}) \\
&\tilde{a}_{kj} := b_j - \frac{b_j}{b_k} a_{jk}, b_j = \tilde{b}_j \\
&\mathbf{k}_1(\mathbf{y}_n, \mathbf{u}_{n_k}) \leq 0 \\
&\mathbf{k}_2(\mathbf{y}_n, \mathbf{u}_{n_k}) \geq 0 \\
&Ecrire\ t_{n+1}, \mathbf{y}_{n+1}, \mathbf{p}_{n+1}
\end{aligned}
\tag{24}
$$

3. Stop.

This algorithm is implemented by A Modeling Language for Mathematical Programming "AMPL". The Nonlinear Interior point Trust Optimization solver

"KNITRO" is called on to extract the optimal dynamic solution of the two-aircraft optimal control problem. The numerical results and the optimality convergence characteristics are presented in the following section.

4 Results and discussion

Figure 1 shows the noise levels when the optimization is applied and the solutions obtained. The observation positions are $(-20000\ m, -20000\ m, 0\ m)$ for $AONL_1$, $(-19800\ m, -19800\ m, 0\ m)$ for $AONL_2$,..., $(-600\ m, -600\ m, 0\ m)$ for $AONL_8$. The touch point on the ground is $(0\ m, 0\ m, 0\ m)$ while the temporal separation of aircraft is 90 s. The observation points are taken on the ground under the flight path and are independent from each other. At each point, it is a vector of N noise levels as shown in the discretization process. It is very important to consider the maximum value among the N values, which value corresponds to the shortest distance between the noise source and the observation point.

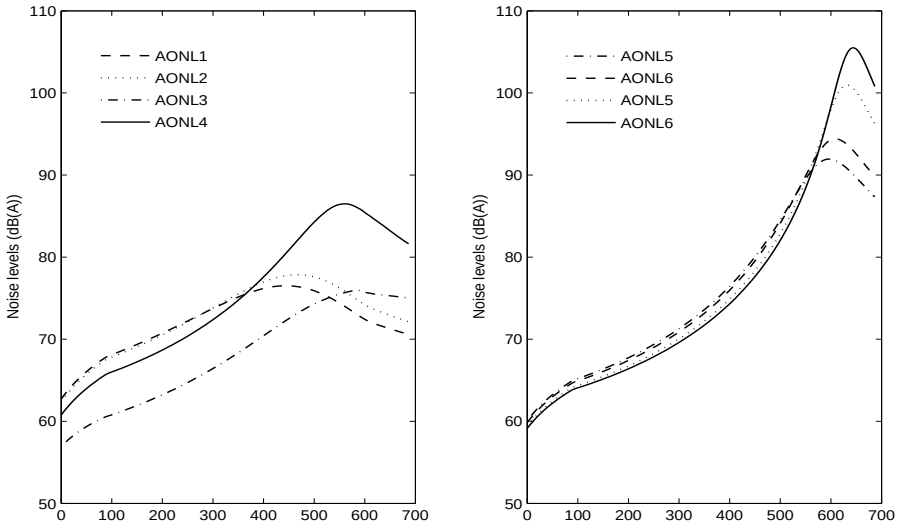


Figure 1: Aircraft noise at the indicated reception point

$AONL$ means Aircraft Optimal Noise Level. As specified, noise levels increase and is maximum when the observation point lies below the aircraft. Noise levels decrease gradually as the aircraft moves away from the observation point. This is in good agreement with [2, 25]. By comparison, this result is also close to standard values of jet noise on approach as shown by Harvey [26, 27]. To conclude, numerical calculations carried out in this paper are efficient and fitted with experimental and theoretical research related to acoustical developments.

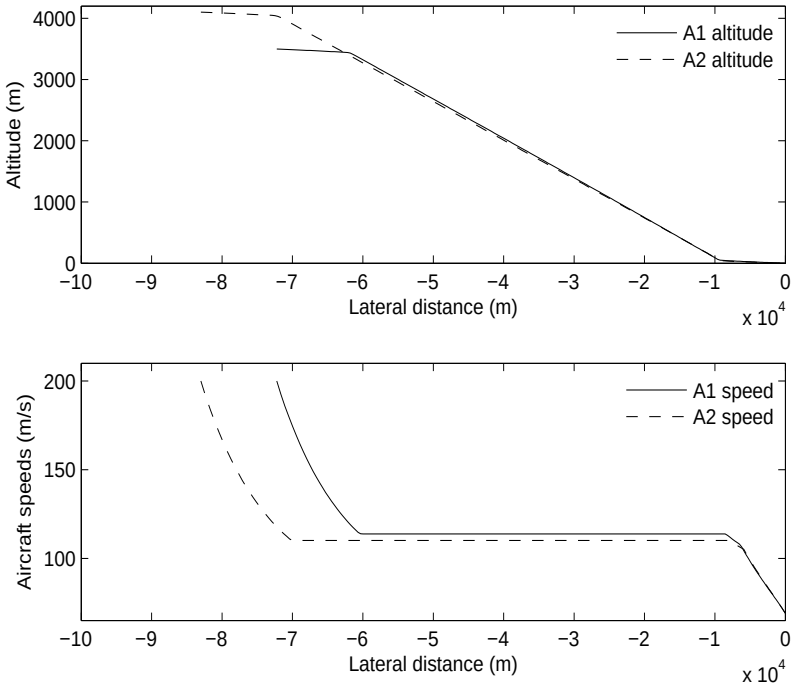


Figure 2: Aircraft optimal flight paths and speeds

Figure 2 shows the trajectories characterized by a part of constant flight level followed by a continuous descent till the aircraft touch point. The aircraft's landing procedures are sufficiently separated. It is obvious that each aircraft follows its optimal trajectory when considering the separation distance. Constraints on speeds described in the previous table are considered, allowing a subsequent landing on the same runway. Thus, as recommended by ICAO, the security conditions are met and flight procedures are good as shown by the presented results. The maximum altitudes considered are 3500 m and 4100 m for the first and second aircraft. The approach duration is 600 s for the first aircraft and 690 s for the second. This figure shows that after some time, the same optimal trajectory have been obtained for the two-aircraft even though the procedures are different. This shows the aircraft trajectory resulting from the two trajectories combination. This figure also shows aircraft speed evolution during landing. For the first, the aircraft speed decreases from 200 m/s to 69 m/s. This evolution remains the same for the speed of the second aircraft.

Figure 3 shows the first aircraft angles versus time as recommended by ICAO. As specified, the aircraft roll angle oscillates around zero. The flight-path angle is negative and bang-bang. It keeps the recommended position for the landing procedures. The attack angle stands between 2° and 20°.

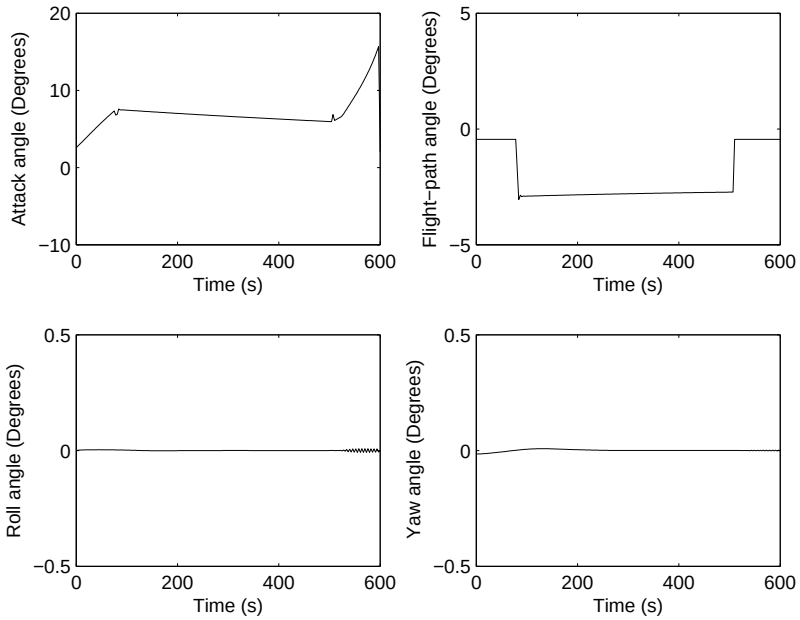


Figure 3: Aircraft flight-path angles

Since the trajectory of the aircraft is aligned with the runway, the yaw angle is small as shown in Figure 3. These angular variations show the aircraft aerodynamic stability and the flight safety.

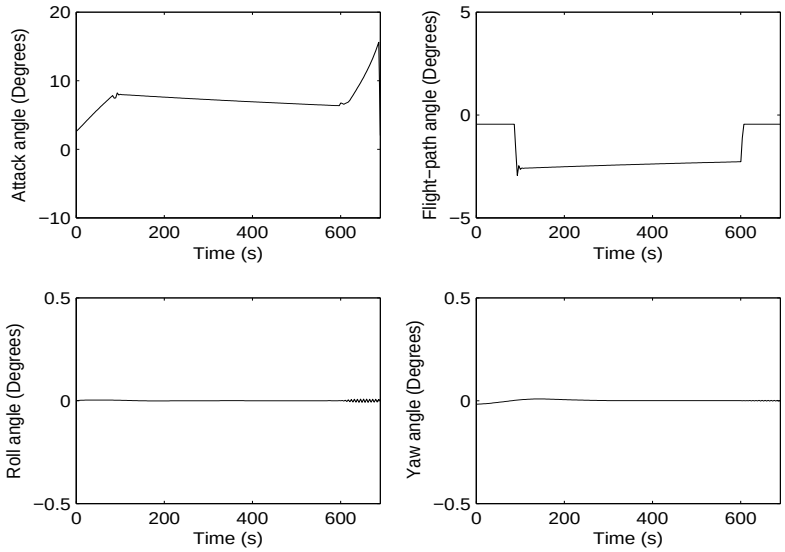


Figure 4: Aircraft flight-path angles

Figure 4 shows the second aircraft angles versus time as recommended by

ICAO during aircraft landing. As specified in this figure, the aircraft roll angle oscillates around zero. The flight-path angle is negative and bang-bang. It keeps also the recommended position for aircraft landing procedures. The attack angle stands between 2° and 20°. Since the trajectory of the aircraft is aligned with the runway, the yaw angle is small as shown in figure 4. These angular variations confirms the aircraft aerodynamic stability and the flight safety.

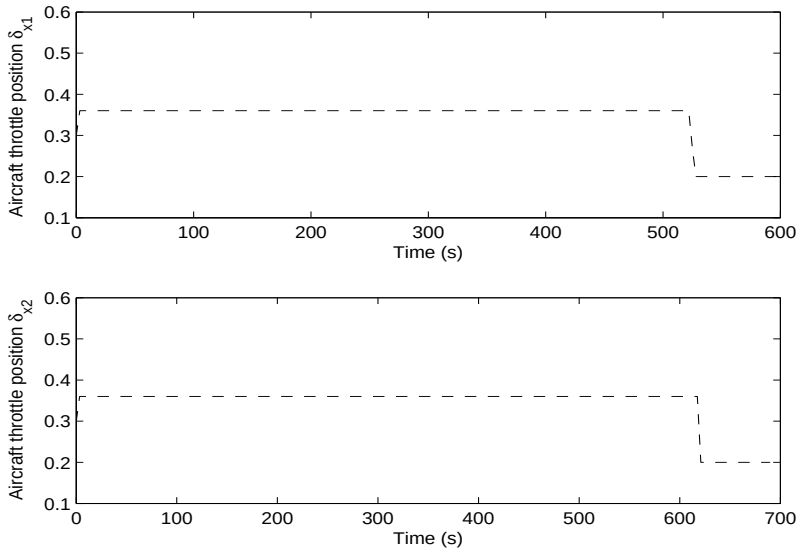


Figure 5: Aircraft throttle variation

Figure 5 shows the aircraft throttle positions during all the approach. They oscillate between 0.2 and 0.6 during the landing procedures. The two-aircraft roll velocity relative to the earth $p_1,\ p_2$, the two-aircraft pitch velocity relative to the earth $q_1,\ q_2$, the two-aircraft yaw velocity relative to the earth $r_1,\ r_2$, the aircraft mass, the roll control, pitch and yaw control reflect the limiters conditions as shown in table 1.

5 Conclusion

In this paper, a mathematical model of two aircraft dynamic system has been developed allowing to reduce noise at the vicinity of airports and to provide suitable optimized flight paths. Theoretical considerations of a symplectic partitioned Runge-Kutta discretization scheme are used. An optimal local solution of the discretized problem is found through a global convergence. Results show a reduction of noise at reception points during the approach of two successive aircraft. The obtained trajectories exhibit optimal characteristics

and are effective where noise reduction is concerned. Further researches are needed for completing the model that will be applied to air traffic.

Acknowledgments. This work is supported by the Agence Universitaire de la Francophonie-Région Afrique Centrale. This is also supported by the French Institute of Science and Technology for Transport, Development and Networks - Transport and Environment Laboratory, Lyon (France).

References

[1] M. Houacine and S.Khardi, Gauss Pseudospectral Method for Less Noise and Fuel Consumption from Aircraft operations, *Journal of Aircraft, Vol.47, No.6, pp.2152-2158,* 2010, ISSN 0021-8669.

[2] S.Khardi L. Abdallah O. Konovalova and M. Houacine, Optimal Approach Minimizing Aircraft Noise and Fuel Consumption, *ACTA ACOUSTICA united with ACUSTICA, The journal of Europian Acoustics Association (EIAA). International Journal on Acoustics,* 2009, ISSN 1610-1928.

[3] E. Roux, Modèle de longueur de piste au décollage-atterrissage, Avions de transport civil, *SUPAERO-ONERA,p 345,* 2006.

[4] I. Chryssoverghi, J. Colestos and B. Kokkinis, Classical and relaxed optimization methods for optimal control problems, *International Mathematical Forum,* 2-2007 N° 30, pp 1477-1498.

[5] A. Fortin, Analyse numérique pour ingénieurs.Troisième edition, *Presses internationales polytechnique,* 2008, ISBN 978-2-553-01427-7.

[6] R-A. Waltz, T-D. Plantenga, KNITRO user's Manual, Version 5.2, *University of Colorado[en ligne]disponible sur http://www.ziena.com*, February, 2008.

[7] R. Fourer, D-M. Gay and B-W. Kernigham, A modelling Language for Mathematical Programming, 2d ed.*Thomson Brooks[en ligne]disponible sur http://www.ampl.com,* 2003

[8] B. Laboratories, AMPL, A modelling Language for Mathematical Programming, *[en ligne]disponible sur http://www.ampl.com,* 2003.

[9] K. Blin, Stochastic conflict detection for air traffic management, *Eurocontrol Experimental centre Publications Office,* France, April 2000.

[10] J-L. Boiffier, The Dynamics of Flight, The Equations, *SUPAÉRO(Ecole Nationale Supérieure de l'Aéronautique et de l'Espace) et ONERA-CERT,* Toulouse 25 Janvier 1999.

[11] E. Roux, Pour une approche analytique de la dynamique du vol, *Thèse, SUPAERO-ONERA*, Novembre 2005.

[12] L. Abdallah, Minimisation des bruits des avions commerciaux sous contraintes physiques et aérodynamique, *Thèse de Mathématiques Appliquées de l'UCBL I,* Septembre 2007.

[13] E. Mary, M-M. Harris, How do we Describe Aircraft Noise? [en ligne] disponible sur www.fican.org , *FICAN*

[14] D. Martin, Noise monitoring in the vicnity of airports, *DSNA-DTI,[electronic] avaible on http://www.dsna-dti.aviation-civile.gouv.fr,* May 2000.

[15] R. James Stone, D.E. Groesbeck and C.L. Zola, An improved prediction method for noise generated by conventional profile coaxial jets, *NASA TM - 82712, AIAA-81-1991,* 1981.

[16] DGAC, Mémento à l'usage des utilisateurs des procédures d'approche et de départ aux instruments, *Rapport de la DGAC, 5ˆème édition,* Août 1995.

[17] DGAC, Méthodes et minimums de séparations des aéronefs aux procédures, *Rapport de la DGAC*, Fevrier 2009.

[18] H. Sors Séparation et contrôle aérien, *International Virtual Aviation Organization[en ligne]disponible sur http://academy.ivao.aero,* 15 octobre 2008.

[19] O. Dominique, Cisaillement de vent ou Windshear, *http://www.aviation-fr.info,* 2008.

[20] J-L Boiffier, Dynamique de vol de l'avion, *SupAéro, Départements des Aéronefs,* Toulouse-Novembre 2001.

[21] Ifrance, Fiches techniques, historiques et photos d'avions A300-600, A300-600R [en ligne]disponible sur http://www.ifrance.com, *Ifrance,*

[22] P. Destunder, Méthodes numériques pour ingénieurs, *Hermes sciences publications*, 12-8-2010.

[23] P. Faurer, Analyse numérique, notes d'optimisation, *Ellipses Marketing,* 1998.

[24] P. Borne, Commande et Optimisation des processus,*Technip,* 17-04-2003

[25] S.Khardi F. Nahayo and M. Haddou, The Trust Region Sequential Quadratic Programming Method Applied to two-Aircraft Acoustic Optimal Control Problem, *Applied Mathematical Sciences, Vol.5, No.40, pp.1953-1976,* 2011, ISSN 1312-885X.

[26] H. Harvey Hubbard, Aeroacoustics of flight vehicles, Theory and Practices, *Volume 1: Noise sources and Volume 2: Noise Control. NASA Langley Research Center,* Hampton, Virginia 1994.

[27] L. Abdallah M. Haddou S. Khardi, Optimization of operational aircraft parameters reducing noise emission, *Applied Mathematical Sciences,* Vol. 4, no 11, 515-535, 2010.

Received: February, 2012

View publication stats